CHAPTER -III

Photoemission calculation with band initial state wavefunction

3.1 Introduction

In the last chapter we have seen that, a simple local model of dielectric function varying with the distance from the surface plane in the surface region gave us a reasonable description of the photocurrent as a function of photon energy for aluminium even with the free electron wavefunction for the initial and the final states. However, we know that we should include the crystal potential for the proper description of the metal - so that we should have the correct band structure and the density of states. In this chapter, we shall take a step in that direction - we shall consider the initial state as a proper band state. We shall describe the final state in the free electron form - although this is not the correct wavefunction. The reason for this is that the computational procedure even with the free electron final state becomes much more involved. We shall give the formalism first and we shall present numerical results for aluminium and show a comparison with the result of the previous chapter. The important results of this chapter have already been published[41].

As before, the main ingredient in the photocurrent calculation is the matrix element $\langle \psi_f | H' | \psi_i \rangle$ where $H' = (e/2mc)(\vec{A}.\vec{p}+\vec{p}.\vec{A})$. For the calculation of ψ_i, we shall assume the solid to be composed of layers parallel to the surface (Fig 3.1); further we shall assume that within each layer there is one atom per unit cell and the centres of all the atoms lie in the same plane parallel to the surface. We shall consider the crystal potential to be of muffin-tin form. For each layer we expand wavefunctions in the muffin-tin form and in the interstitial region, since the potential is constant the wavefunctions can be expanded into forward and backward travelling plane waves. With the centre of a muffin tin sphere in the layer chosen as origin, the

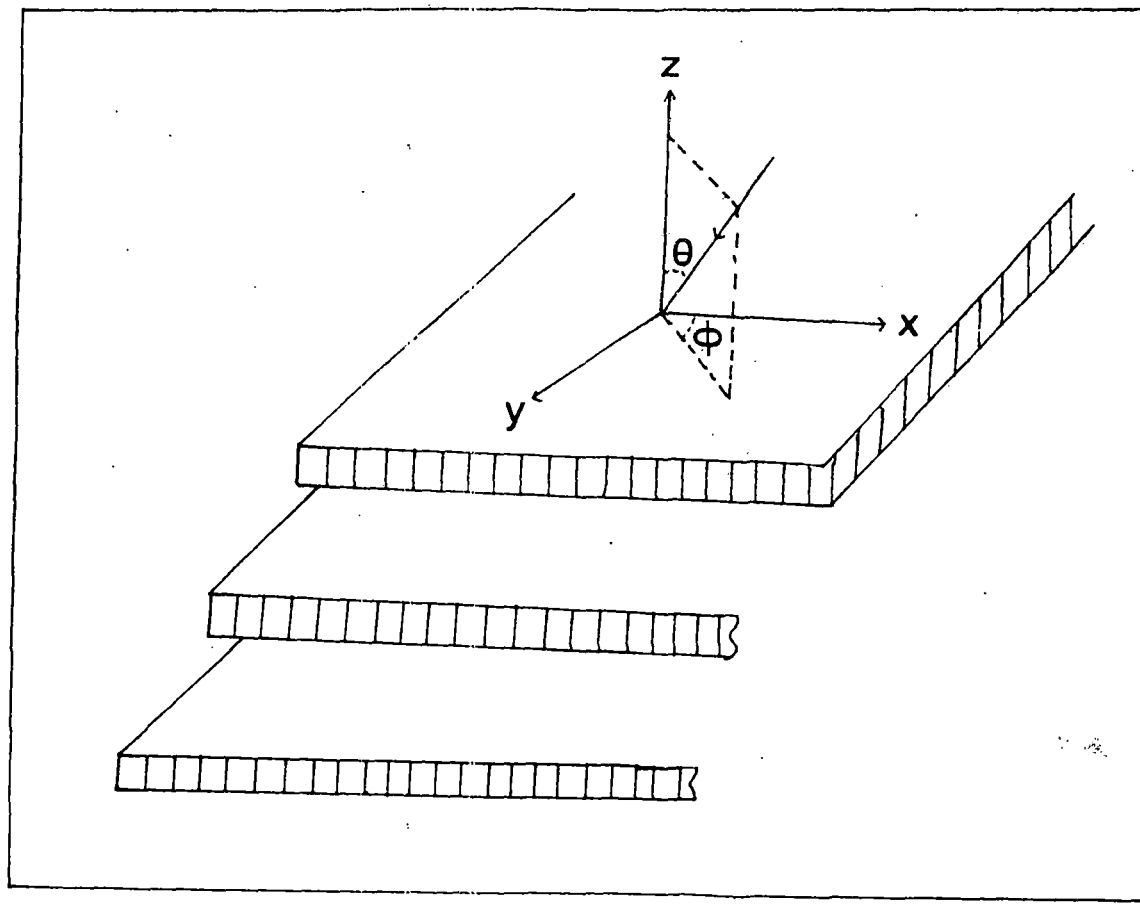

Fig 3.1 Schematic view of the crystal, considered as a stack of layers of atoms parallel to the surface

wavefunction may be written as:

$$\psi_i(\vec{r}) = \begin{cases} \sum_L A_{1L} f_{1l}(R)\, Y_L(\theta,\phi) & \text{spherical region} \\ \sum_{\vec{g}} [u_{\vec{g}} e^{i\vec{k}_{\vec{g}}^{+}\cdot\vec{R}} + v_{\vec{g}} e^{i\vec{k}_{\vec{g}}^{-}\cdot\vec{R}}] & \text{interstitial region} \end{cases}$$

$$\text{where, } \vec{K}_{\vec{g}}^{\pm} = \left[(\vec{k}+\vec{g})_{\parallel}, \pm\sqrt{2(E_i - V_0) - |\vec{k}+\vec{g}|_{\parallel}^2} \right], \quad \text{and} \quad \vec{R} = \vec{r} - \vec{c}_j \tag{3.1}$$

with the $\vec{g}$'s denoting two-dimensional reciprocal lattice vectors and $\vec{c}_j$ is the origin at the j-th layer. V_0 is the constant interstitial potential with respect to vacuum. To determine $u_{\vec{g}}$ and $v_{\vec{g}}$ an eigenvalue equation is constructed by using scattering properties of the layer and the Bloch condition, the solutions of which give the Bloch waves with the real and complex wave vectors. From these, the real Bloch waves propagating towards the surface are identified. $u_{\vec{g}}$ and $v_{\vec{g}}$ form the eigenvector for this Bloch wave. The construction of the eigenvalue equation is given in the appendix-I. The $u_{\vec{g}}$, $v_{\vec{g}}$'s corresponding to different layers are related by Bloch equation. This method is used in LEED type calculations and the details are given , for example, by Pendry[36]. The A_L's are determined from $u_{\vec{g}}$'s and $v_{\vec{g}}$'s by proper matching.

With the wavefunctions in each layer thus determined, one can write down the initial state wavefunction in the vacuum region as an exponentially decaying function

$$\psi_i(\vec{r}) = \sum_{\vec{g}} T_{\vec{g}} e^{i\vec{K}_{\vec{g}}\cdot(\vec{r}-\vec{r}_0)_{\parallel}} e^{-\chi_{\vec{g}}(z-z_0)} \quad \text{vacuum region}$$

$$\text{where,} \quad \chi_{\vec{g}} = \sqrt{-[2E_i - (k+\vec{g})_{\parallel}^2]} \tag{3.2}$$

and $z=z_0$ is the surface plane with respect to the origin in the first

layer. The coefficient $T_{\vec{g}}$ can determined by matching across the vacuum plane.

The final state ψ_f and the vector potential $\vec{A}$ are taken to be the same as in the last chapter. This means that we shall be considering p-polarized radiation in the long wavelength limit, and only the z-component (i.e., the one normal to the surface) will be considered. In addition, since in the description of the initial state the solid is divided up into layers, we shall consider the surface region to be equal to an integral number of layers. In what follows, we shall take the surface region to be the same as the first layer for calculational simplicity, but this may be extended to include more than one layer.

3.2 Matrix element calculation

We may now write down the matrix element for the solid as a whole

$$\langle \psi_f | H' | \psi_i \rangle = \int_{vac} \psi_f^* H' \psi_i \, d^3r + \int_{1st} \psi_f^* H' \psi_i \, d^3r + \sum_j \int_{bulk} \psi_f^* H' \psi_i \, d^3r \tag{3.3}$$

where, in each region the wavefunctions and vector potentials corresponding to that region have to be used.

i] Vacuum region

For this region form of the wavefunctions and the photon field are as follows

$$\psi_i(\vec{r}) = \sum_{\vec{g}} T_{\vec{g}} e^{i\vec{K}_g \cdot (\vec{r}-\vec{r}_0)} e^{-\chi_g (z-z_0)}$$

$$\psi_f(\vec{r}) = e^{i\vec{q} \cdot (\vec{r}-\vec{r}_0)} + \frac{q-k_f}{q+k_f} e^{-i\vec{q} \cdot (\vec{r}-\vec{r}_0)}$$

$$A_\omega(z) = A_1 \epsilon(\omega)$$

and the integration can be calculated analytically and the result is

$$T_1 = \int_{z_0}^{\infty} \psi_f^* \vec{A}_\omega . \vec{\nabla} \psi_i \, d^3 r$$

$$= -A_1 \epsilon \chi_0 T_0 S_0 \left[\frac{1}{\chi_0 + iq} + \frac{q - k_f}{q + k_f} \frac{1}{\chi_0 - iq} \right]$$

(3.4)

where, S_0 is the area of the surface unit cell. The integration for the parallel part becomes a δ-function from which we get only the contribution from the term $\vec{g}=0$.

ii] First (surface) layer

We have taken the width of the surface layer to be different from the other layers. This was done so that the metal-vacuum interface ($z=z_0$) can be taken to be tangential to the last layer of muffin-tin spheres as shown in fig 3.2. The form of the photon field in the surface layer is

$$A_\omega(z) = \frac{A_1 \epsilon(\omega)}{[1-\epsilon(\omega)]\,(\frac{z}{a}+\beta_1)} \quad \text{with} \quad \beta_1 = \frac{1}{[1-\epsilon(\omega)]} - \frac{z_0}{a}$$

In the factor β_1, which is similar to B_1 of the chapter-II, an additional term $(-z_0/a)$ comes due to the change in the position of the origin. Here we have taken the muffin-tin centre as the origin instead of the metal vacuum interface as considered in the previous chapter.

In each layer we shall calculate the matrix element for the interstitial and muffin-tin region separately.

The evaluations of the integral over the interstitial region is somewhat more complicated because of the shape of the region. To do it, we perform the integration over the cell (whole layer) and over the muffin-tin sphere, using the form for ψ_i for the interstitial region. Subtracting these two integrals we obtain the matrix element for

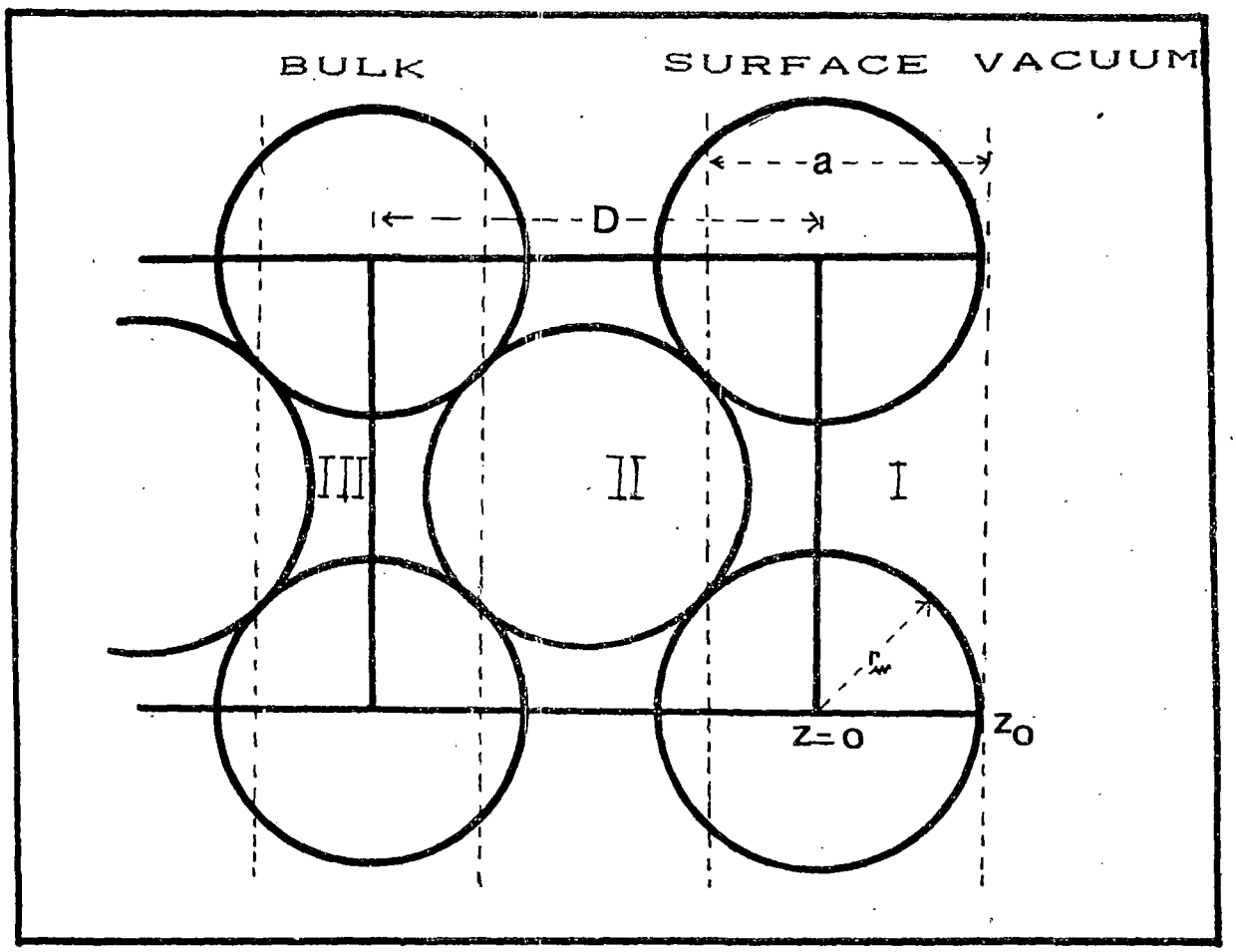

Fig 3.2 View of the muffin-tin potential at the surface of a solid

the interstitial region as given in the following equation

$$\int_{inst} \psi_f^* H' \psi_i d^3r = \int_{cell} \psi_f^* H' \psi_i d^3r - \int_{mft} \psi_f^* H' \psi_i d^3r$$

(3.5)

In the interstitial region the wave functions have the following form

$$\psi_f(\vec{r}) = \frac{2q}{q+k_f} e^{ik_f(\vec{r}-\vec{r}_0)}$$

$$\psi_i(\vec{r}) = \sum_{\vec{g}} \left[u_{\vec{g}} e^{ik_{\vec{g}}^+ \cdot \vec{r}} + v_{\vec{g}} e^{ik_{\vec{g}}^- \cdot \vec{r}} \right]$$

Using the above forms for the wave functions we calculate the integration over the cell as

$$T_2 = \int_{-\frac{D}{4}}^{z_0} \psi_f^* \left[\vec{A}_\omega \cdot \vec{\nabla} + \frac{1}{2} (\vec{\nabla} \cdot \vec{A}) \right] \psi_i d^3r$$

$$= p_1 S_0 \int_{-\frac{D}{4}}^{z_0} \left[\frac{iK_{\vec{g}z}^+}{\frac{z}{a}+\beta_1} \left\{ u_0 e^{iK_{\vec{g}fz}^+ z} - v_0 e^{iK_{\vec{g}fz}^- z} \right\} \right.$$

$$\left. - \frac{1}{2a(\frac{z}{a}+\beta_1)^2} \left\{ u_0 e^{iK_{\vec{g}fz}^+ z} + v_0 e^{iK_{\vec{g}fz}^- z} \right\} \right] dz$$

$$\text{where, } p_1 = \frac{2qA_1 \epsilon e^{i\vec{k}_f \cdot \vec{r}_0}}{(q+k_f)(1-\epsilon)} \text{ and } \vec{K}_{\vec{g}f}^{\pm} = \vec{K}_{\vec{g}}^{\pm} - \vec{k}_f$$

(3.6)

and D is the lattice constant.

For evaluating the integral over the muffin-tin sphere, we have to expand ψ_f , ψ_i and the z-component of the vector potential in spherical harmonics (or Legendre Polynomials). To express A_z and A_z' in

spherical coordinate, we write them in the following form

$$A_\omega(z) = A_\omega(r\cos\theta) = \frac{1}{\frac{r}{a}\cos\theta+\beta_1} = \sum_l B_l(r)\, P_l(\cos\theta)$$

$$\text{with } B_l(r) = \frac{2}{2l+1}\int_0^\pi A_\omega(r\cos\theta)\, P_l(\cos\theta)\sin\theta\, d\theta$$

$$\text{and } A'_\omega(z) = A'_\omega(r\cos\theta) = \frac{1}{\left(\frac{r}{a}\cos\theta+\beta_1\right)^2} = \sum_l D_l(r)\, P_l(\cos\theta)$$

$$\text{with } D_l(r) = \frac{2}{(2l+1)}\int_0^\pi A'_\omega(r\cos\theta)\, P_l(\cos\theta)\sin\theta d\theta$$

(3.7)

We have calculated these integrals analytically using the standard form of the integrations[42]. The details of the expressions for the radial part of the photon field $B_l(r)$ and $D_l(r)$ for different values of angular momentum l are given in the Appendix-I.

We calculate the matrix element in the muffin-tin region using the interstitial form for the initial state wavefunction given by

$$T_3 = \int_0^{r_m} \psi_f^* \left[\vec{A}_\omega . \vec{\nabla} + \frac{1}{2} (\vec{\nabla} . \vec{A}_\omega) \right] \psi_i \, d^3 r$$

$$= 8\pi p_1 \sum_{\vec{g},l} \frac{i^l}{2l+1} \Big[\Big\{ i K_{gz}^+ \int_0^{r_m} [u_{\vec{g}} P_l(K_p^+) j_l(|\vec{K}_{\vec{g}f}^+| r)$$

$$- v_{\vec{g}} P_l(K_p^-) j_l(|\vec{K}_{\vec{g}f}^-| r)] B_l(r) r^2 dr \Big\}$$

$$- \Big\{ \frac{1}{2a} \int_0^{r_m} [u_{\vec{g}} P_l(K_p^+) j_l(|\vec{K}_{\vec{g}f}^+| r)$$

$$+ v_{\vec{g}} P_l(K_p^-) j_l(|\vec{K}_{\vec{g}f}^-| r) D_l(r) r^2 dr \Big\} \Big]$$

$$\text{where, } K_p^\pm = \vec{K}_{\vec{g}f}^\pm . \hat{z}$$

(3.8)

and r_m being the muffin-tin radius. Here we have used the standard expansion

$$e^{i\vec{k}^\pm . \vec{r}} = 4\pi \sum_L i^l j_l(|\vec{K}^\pm| r) \, Y_L(\vec{r}) \, Y_L^*(\vec{K}^\pm)$$

(3.9)

and also the orthogonality properties of spherical harmonics.

The form for the initial state wave function inside the muffin-tin sphere is given by

$$\psi_i(\vec{r}) = \sum_L A_L f_l(r) \, Y_L(\theta, \phi)$$

and the calculated form of the matrix element over the muffin-tin sphere comes out to be

$$T_4 = \int_0^{r_m} \psi_f^* \left[\vec{A}_\omega . \vec{\nabla} + \frac{1}{2} (\vec{\nabla} . \vec{A}_\omega) \right] \psi_i \, d^3 r$$

$$= 8\pi p_1 \sum_{L_1, l_2, L_3} \frac{A_{L_3} (-i)^{l_1} Y_{L_1} (\vec{k}_f)}{2 l_2 + 1} \int_0^{r_m} \left[\left\{ C^1_{L_1 l_2 L_3} \left[\frac{\partial}{\partial r} f_{L_3} (r) \right] r^2 \right.\right.$$

$$\left.\left. + C^2_{L_1 l_2 L_3} f_{l_3} (r) \, r \right\} B_{l_2} (r) - \frac{1}{2a} C^3_{L_1 l_2 L_3} f_{l_2} (r) \, r^2 D_{l_2} (r) \right] j_{l_1} (k_f r) \, dr$$

(3.10)

Although the explicit form of the equations (3.8 & 3.10) are the same but we have used different form for ψ_i. In the above equation angular parts of the integration are given by

$$C^1_{L_1 l_2 L_3} = \int_\Omega Y_{L_1}^* \, Y_{L_3} \, P_{l_2} (\cos\theta) \cos\theta \, d\Omega$$

$$C^2_{L_1 l_2 L_3} = \int_\Omega Y_{L_1}^* P_{l_2} (\cos\theta) \left[\frac{\partial}{\partial \theta} Y_{L_3} \right] Sin\theta \, d\Omega$$

$$C^3_{L_1 l_2 L_3} = \int_\Omega Y_{L_1}^* P_{l_2} (\cos\theta) \, Y_{L_3} \, d\Omega$$

For further simplifications for these angular integrals we have used the recursion relations for the spherical harmonics.

Therefore, 1st layer contribution to the matrix element can be calculated from the terms T_2, T_3 and T_4 and equation (3.5) as $T_5 = T_2 - T_3 + T_4$

iii] Bulk layers

For the bulk layers we calculate the matrix element over the interstitial and muffin-tin region separately as we have done in the 1st layer. It is to be noted that the photon field is constant here given by

$$A_\omega (z) = A_1$$

and in the integration we have no term involving the variation A(z). In the bulk layers the calculations are simpler compared to that of the 1st layer and we have calculated some of terms analytically.

Term T_5 is the matrix element for the cell (whole layer) with the interstitial form for the initial state wavefunction, similar to the term T_2 of the 1st layer given by

$$T_5 = p_2 S_0 K_{gz}^{+} \left[\frac{u_0 \sin\left[K_{gfz}^{+} \frac{D}{4}\right]}{K_{gfz}^{+}} - \frac{v_0 \sin\left[K_{gfz}^{-} \frac{D}{4}\right]}{K_{gfz}^{-}} \right]$$

$$\text{where,} \quad p_2 = \frac{2iqA_1 e^{i\vec{k}_f \cdot \vec{r}_0}}{(q+k_f)}$$

(3.11)

Similarly, in the interstitial we calculate term T_6 which is identical to term T_3 of the surface layer

$$T_6 = 8\pi\sqrt{\pi} p_2 \sum_{g} K_{gz}^{+} \int_0^{r_m} \left[u_g j_0\left(|\vec{K}_{gf}^{+}|R\right) Y_0^{*}\left(\vec{K}_{gf}^{+}\right) \right.$$

$$\left. - v_g j_0\left(|\vec{K}_{gf}^{-}|R\right) Y_0^{*}\left(\vec{K}_{gf}^{-}\right) \right] R^2 dR$$

(3.12)

Calculation of the matrix element in the muffin-tin region is the same as in the surface layer (term T_4) and the result comes out to be

$$T_7 = p_3 \sum_{L_1 L_3} (-i)^{l_1} A_{L_3} Y_{L_1}(\vec{k}_f) \left[\int_0^{r_m} \left\{ C^4_{L_1 L_3} \left(\frac{\partial}{\partial R} f_{l_3}(R) \right) R^2 \right.\right.$$

$$\left.\left. - C^5_{L_1 L_3} f_{l_3}(R) R \right\} j_{l_1}(|\vec{k}_f| R)\, dR \right]$$

where, $$C^4_{L_1 L_3} = \int_\Omega Y_{L_1}^* Y_{L_3} \cos\theta \, d\Omega$$

$$C^5_{L_1 L_3} = \int_\Omega Y_{L_1 L_3}^* \left[\frac{\partial}{\partial \theta} Y_{L_3} \right] \sin\theta \, d\Omega$$

$$and \quad p_3 = -i p_2 8\pi^2$$

(3.13)

Similar to the surface layer the bulk contribution (using equation 3.5) is obtained from the relation $T_B = T_5 - T_6 + T_7$.

Using the values for the different terms T_S, T_B and $T_V (= T_1)$ we have calculated the photoemission cross-section numerically (using eqn.3.3) for which some portions of the FORTRAN programs are given in the appendix-III.

3.3 Results and discussion

We have applied our formalism to calculate normal photoemission cross-section from the Fermi level of aluminium and tungsten as a function of photon energy. For both the structures we have calculated the band structures where the imaginary part of the crystal potential has been taken to be zero. We have used some of the subroutines given by Pendry[36] and Hopkinson *et al* [43]. For the photon field calculation, data given by Weaver[35] for the complex dielectric function of aluminium and tungsten as a function of photon energy were used. The maximum value of the angular momentum L has been taken to be 4. Since the final state was taken to be free electron like a convergence factor of $\exp(-\alpha z)$ was

introduced in the final state to take into account the inelastic scattering of electrons.

The muffin-tin potential and the crystal parameters for aluminium are those given by Pendry[36]. We have taken[37] E_f=11.7 ev, V_0=15.95 ev and the lattice constant for aluminium as 4.05 A^0. In the figure (3.3), we show the result obtained for normal photoemission ($\vec{k}_{\parallel}$=0) for a p-polarised photon incident at 45^0 to the surface normal. The two curves shown correspond to two different values for the parameter '*a*' defining the surface region in the field calculation. The curve (I) is for '*a*' taken to be the same as the first layer while the plot (II) is for '*a*' equal to the first two layers. The scale for photocurrent for the two curves are not the same - we have plotted them so that the peaks around 11 ev are of comparable height. The value of α was taken to be 0.35 (the same value used earlier with free electron initial & final states in chapter-II).

The calculated photocurrent[41] shows a peak at 11.5 eV followed by a minimum at the plasmon energy (~16 eV) and a broad maximum around 20 eV. We have seen that these features are also present in the experimentally observed and previously calculated results[20,22] (fig. 2.3). In fig 3.4 we have compared the photocurrent variation against the photon field for the two types of crystal potential: muffin-tin (I) and free-electron (II). The scale of the photocurrent in the two curves are different but we have plotted them so that the peaks around 11 eV are of comparable height. Fig 3.4 shows that the ratio of the peak heights of the two peaks (below and above the plasmon energy) are of the order of 15 (free electron potential) and 3.6 (muffin-tin potential with a= thickness of first layer only) but in the experimental curve this ratio

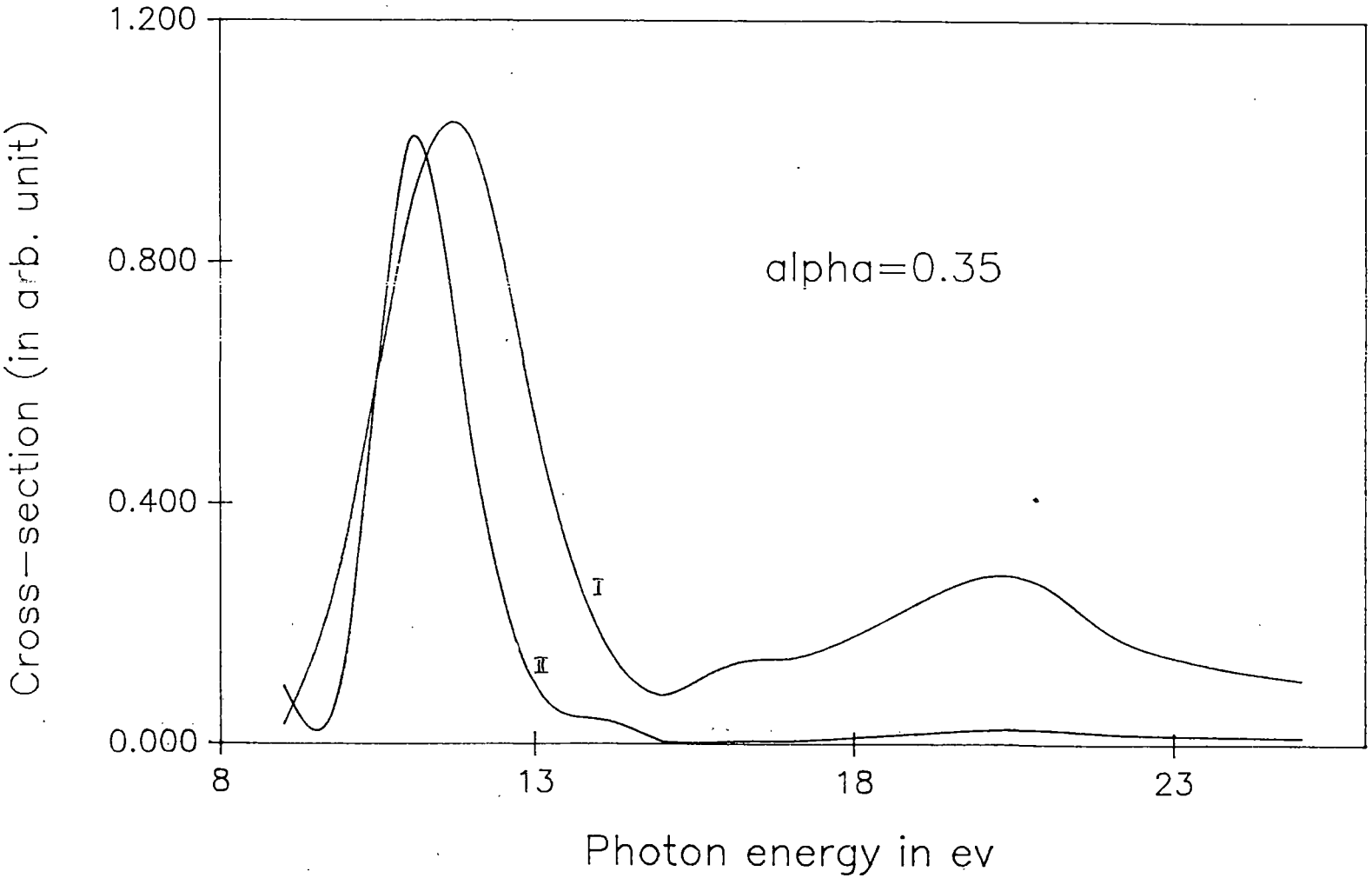

Fig 3.3 Calculated photocurrent against photon energy for normal emission from the Fermi level of aluminium (100) face with the surface region for field variation, a = thickness of the first layer (I) and first two layers (II)

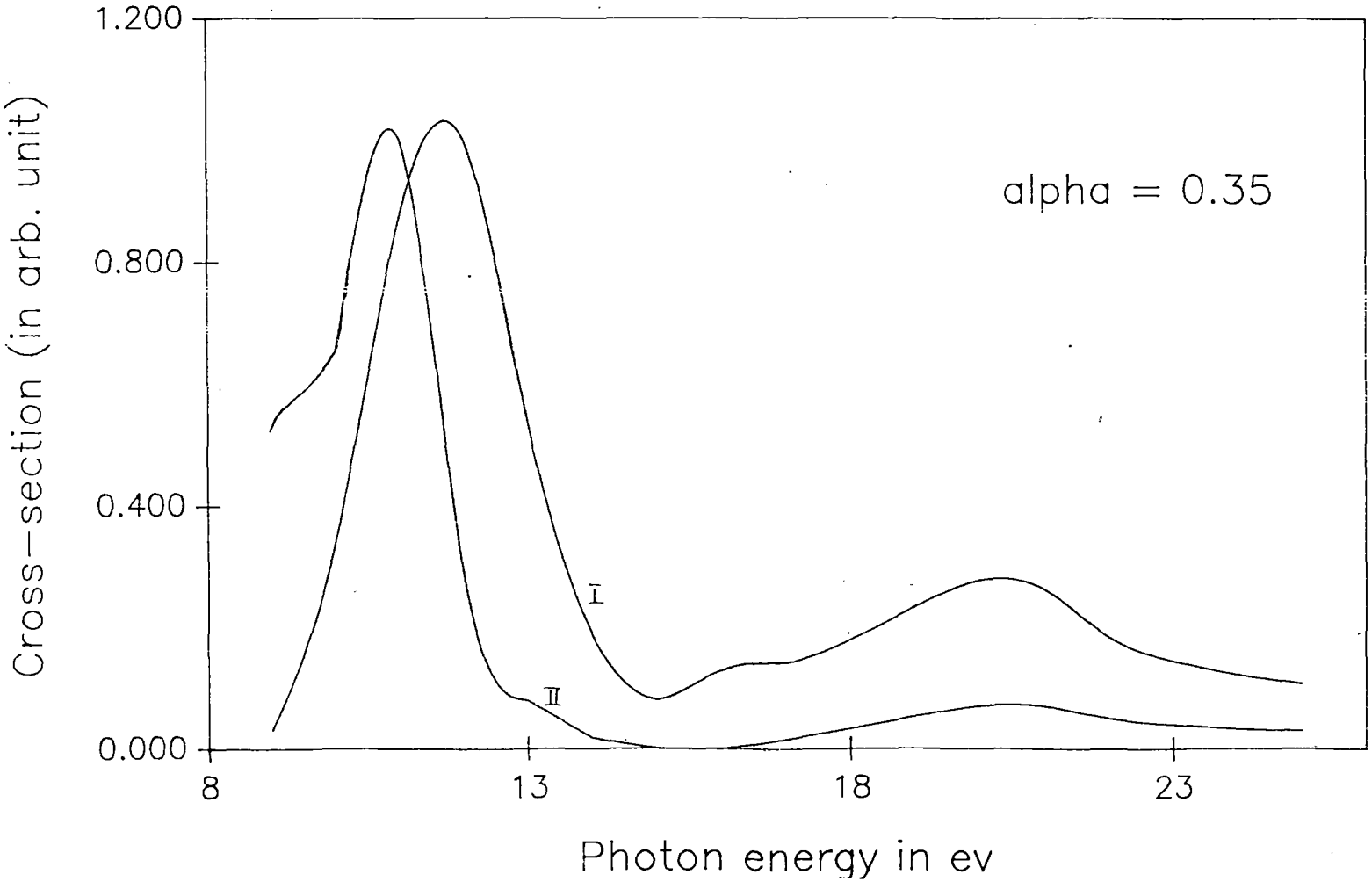

Fig 3.4 Photocurrent versus photon energy for two types: muffin-tin (I) and free-electron (II) potential for aluminium

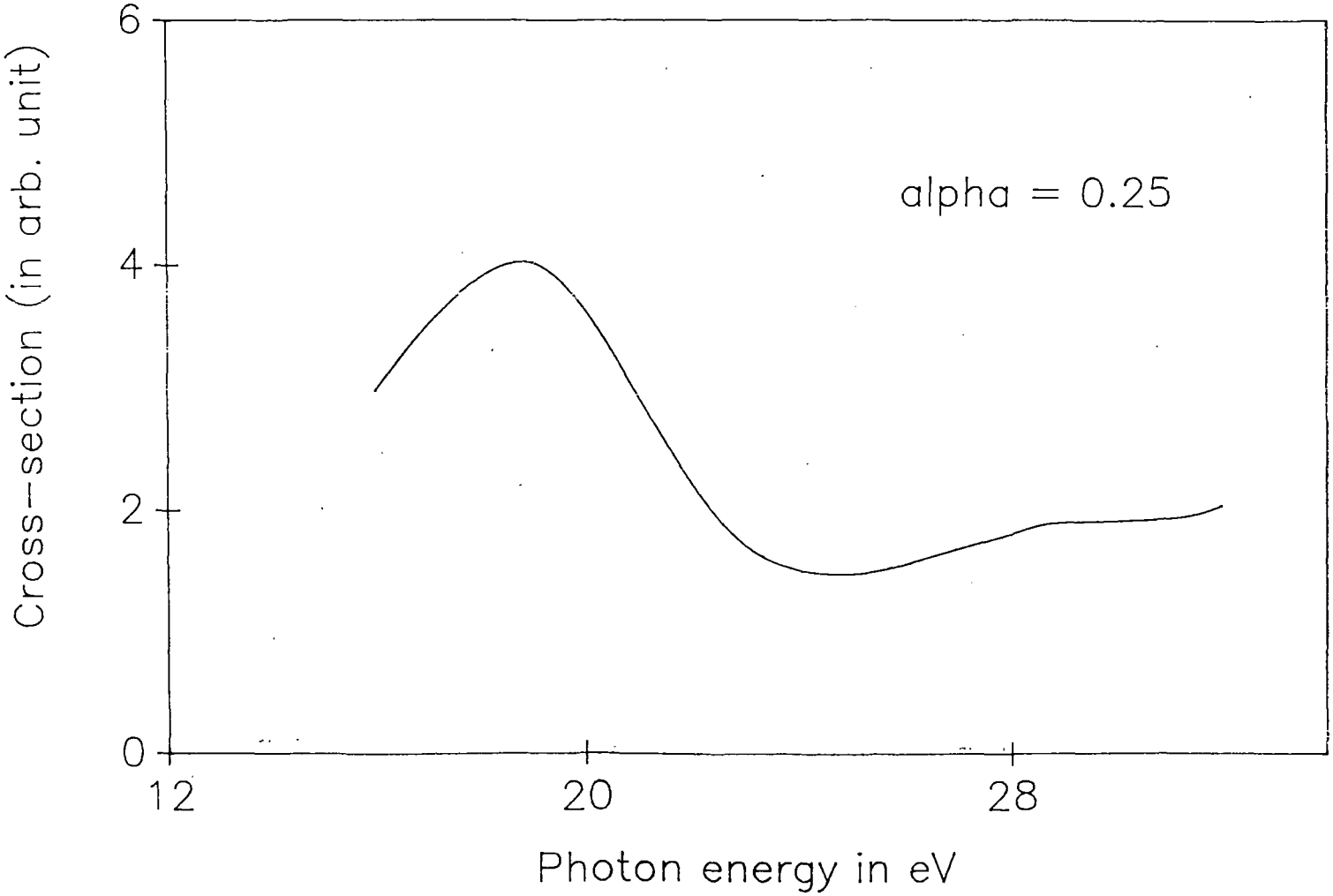

Fig 3.5 Photocurrent against photon energy for normal photoemission from tungsten (100) face

is of the order of 6. Again, if we consider *a* to be equal to the thickness of the first two layers this ratio comes out to be ~23 (curve II in fig 3.3). From the fig.3.3 it is evident that the field variation may be taken to be over the first layer only - at least with this model.

As a further application of our formalism we have considered a bcc lattice (tungsten). For the potential and the other crystal parameters of tungsten we have used the data given by Matheiss[44]. The lattice constant of tungsten is 3.16 A^{0}[37]. For the non-relativistic band structure as given by Matheiss[41], there is no Δ_1 at the Fermi energy, and it is known[42] that the only Δ_1 states can contribute to photocurrent for normal emission when p-polarised radiation is used. We have considered, the current from the Δ_1 band edge about 4 eV below the Fermi level.

Our calculated photoemission cross-section for tungsten as a function of photon energy (fig 3.5) shows a peak around 18 eV and a minima near the plasmon energy (24-25 eV), which is to be expected. It is also seen that the Δ_2 band at that energy makes a negligible contribution to current. However, for tungsten, relativistic spin-orbit effects are also important, so this calculation may be regarded as an example of calculation with bcc crystals.

So, we may conclude that use of band wavefunctions gives better agreement compared to previous calculations with free electron wavefunctions.